Origin of nanoscale potential fluctuations in two-dimensional semiconductors

S. Landrock, Y. Jiang, K. H. Wu, E. G. Wang, K. Urban, and Ph. Ebert

Citation: Appl. Phys. Lett. **95**, 072107 (2009);
View online: https://doi.org/10.1063/1.3177329
View Table of Contents: http://aip.scitation.org/toc/apl/95/7
Published by the American Institute of Physics

Origin of nanoscale potential fluctuations in two-dimensional semiconductors

S. Landrock,[1] Y. Jiang,[1,2] K. H. Wu,[2] E. G. Wang,[2] K. Urban,[1] and Ph. Ebert[1,a)]
[1]*Institut für Festkörperforschung, Forschungszentrum Jülich GmbH, 52425 Jülich, Germany*
[2]*Institute of Physics, Chinese Academy of Science, Beijing 100080, People's Republic of China*

(Received 13 May 2009; accepted 24 June 2009; published online 19 August 2009)

We demonstrate a direct atomically resolved visualization and quantification of the impact of inhomogeneities in the dopant distribution on the nanoscale potential fluctuations in a two-dimensional semiconducting $\sqrt{3}\times\sqrt{3}$ Ga overlayer on Si(111) using scanning tunneling microscopy. By a quantitative analysis, two regimes of the potential at nanometer scale are found, which arise from the local distribution of charge carriers in the bands and from electron-electron interactions. © *2009 American Institute of Physics*. [DOI: 10.1063/1.3177329]

With the ongoing push for smaller semiconductor devices, the feature size implemented in current commercial manufacturing processes is reaching dimensions, where ultimately the device operation depends on a single electron and traditional device concepts break down. In such conditions, statistical fluctuations in the dopant distribution become particularly important.[1,2] Inhomogeneities in the dopant distribution[3] may cause nanoscale and atomic-scale fluctuations in the potential,[4] which in turn would lead to a statistical lowering of the threshold voltages.[1] However, in other cases, no effect of the spatial positions of charged defects on the local potential was found.[5] This inconsistency is essentially due to the lack of solid experimentally proven facts about the effect of nanoscale dopant inhomogeneities on the *local* nanoscale and atomic-scale potential. It is still unclear which physical mechanisms determine the nano- and atomic-scale potential and which quantitative models can be used for accurate simulations of the potential in spatially (and/or dimensionally) reduced semiconductor structures.

Therefore, we illustrate here a direct atomically resolved visualization and quantification how dopant atoms and their statistical distribution affect the local nanoscale and atomic-scale potential using scanning tunneling microscopy (STM). We identify two different origins of the nanoscale potential and derive a quantitative physical understanding of dopant-induced potential fluctuations at nanometer and subnanometer scales.

As a model system, we utilize a two-dimensional (2D) $\sqrt{3}\times\sqrt{3}$ Ga on Si(111) structure, where we can tune the dopant concentration over a wide range by suitable adjustment of the deposition parameters. Figure 1(a) shows an atomically resolved *constant-current* STM image of our model system: each maximum in the empty state STM image corresponds to one empty dangling bond above a Ga adatom. The weaker maxima (marked D), whose concentration decreases with increasing Ga deposition, arise from Si atoms located on $\sqrt{3}\times\sqrt{3}$ Ga sites.[6] These Si atoms act as donors and provide the free electrons.[7] The resulting positive charges of the Si dopants induce a redistribution of the free charge carriers and thereby a potential change, which gives rise to the surrounding bright contrast on which the atomic corrugation is superimposed.[8] The local potential change also shows up in the tunneling spectra: the valence (E_V) and conduction band (CB) edges (E_C) shift ≈0.15 eV to higher energies with increasing spatial separation from the dopant site [dotted lines in Fig. 1(c)].

In addition, the STM images exhibit long-range height changes with lateral extensions of 5–15 nm [see dashed and dotted elliptical lines in Fig. 1(a)]. The above observed band-edge shifts indicate again that potential changes along the surface give rise to the long-range height changes in STM images. Furthermore, regions with dark and bright contrast appear in surface areas with low and high dopant concentration, respectively. This observation is corroborated by the quantitative analysis of the local height change Δz in the STM image (i.e., defined as deviation from the spatial average z_{avg} of tip-sample separation $z=z_{\mathrm{avg}}+\Delta z$) as a function of the local dopant concentration n_{local} [analyzed in circular areas with the diameter defining the resolution in Fig. 2(a)]. Note that we only consider the average height and not the superimposed atomic corrugation, which is a local density of states (DOS) effect not related to the potential. Δz increases with the local dopant concentration.

The trend in Fig. 2(a) can be explained quantitatively by potential fluctuations. The tunnel current, and thereby the height in constant-current images, is related to the local potential $U=E_C-E_F$, with E_F being the constant Fermi energy [Fig. 2(c)]. The Δz scale is transformed into a potential (ΔU) scale following a modified version of the methodology of Ref. 9.

(i) First, by measuring a height-voltage (Z-V) curve at constant current with identical tip configuration [inset in Fig. 2(a)], the Δz scale can be transformed into an equivalent voltage scale, and a voltage image is obtained by $\Delta V=S^{-1}\Delta z$, with the voltage sensitivity $S=\partial Z/\partial V|_{V_0}$ of the respective tip at the set voltage V_0 during measurement.

(ii) Second, the relationship of the voltage and potential scales can be determined from the tunnel current I given at positive sample voltages V by the *integral* over all sample states (with an energy $\varepsilon \geq E_F \equiv 0$) into which electrons can tunnel [Fig. 2(c)].[10]

$$I(V,U) \propto \int_0^{eV} \rho(\varepsilon)\cdot e^{-2z\sqrt{(2m_0/\hbar^2)[\bar{\Phi}(U)+(eV/2)-\varepsilon]}}d\varepsilon. \qquad (1)$$

$\bar{\Phi}(U)$ is the average work function of the tip Φ_T and the sample $\Phi_S=\chi+U$ (χ electron affinity), m_0 the electron mass, and ρ is the surface DOS, which is zero in the surface band

a)Electronic mail: p.ebert@fz-juelich.de.

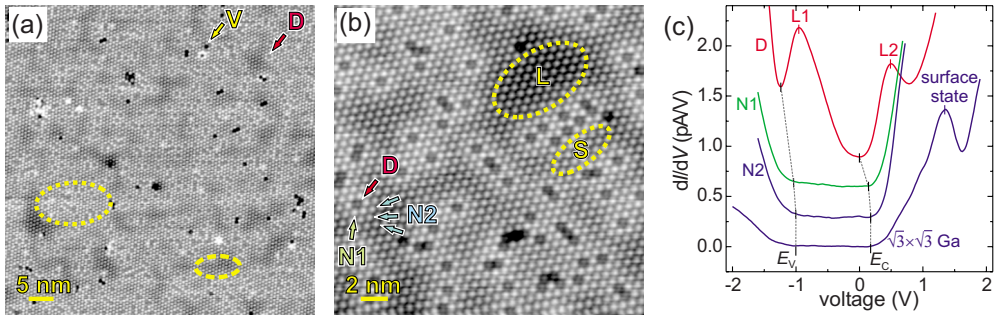

FIG. 1. (Color online) (a) STM image of a 2D semiconducting $\sqrt{3}\times\sqrt{3}$ Ga overlayer on Si(111) measured at 2 V. In addition to atomic-sized features arising from vacancies (V) and Si dopant atoms (D), long-range changes in the contrast occur. Examples are indicated by dashed (depression) and dotted (elevation) elliptical lines. (b) High-resolution STM image. Each charged Si dopant is surrounded by a bright contrast. (c) dI/dV tunneling spectra above dopants (D), directly neighboring Ga atoms (N1), Ga atoms further away (N2) [(see (b)], and for the $\sqrt{3}\times\sqrt{3}$ Ga overlayer (all Ga sites not neighboring to dopants). For enhanced sensitivity, the spectra D, N1, and N2 were taken at a tip-sample separation 0.06 nm smaller and each curve is offset by 0.3 pA/V for clarity. The conduction (E_C) and valence (E_V) band edges shifts are indicated by a dotted line. L1 and L2 are localized states related to the Si donors.

gap. The DOS of the tip is assumed to be constant and is included in the proportionality constant. The exponent in Eq. (1) describes that electrons tunneling with an energy ε feel an effective barrier of $\bar{\Phi}+(eV/2)-\varepsilon$. Equation (1) yields identical currents for either a small potential change $\Delta U=\Delta E_C$ or a small change $-e\Delta V$ of the voltage,[11] since the barriers and integration ranges are identical in both cases, as illustrated graphically in Fig. 2(c). Thus, with $\Delta U=-e\Delta V$ we obtain in Fig. 2(a), the relationship between the local potential (left axis) and local dopant concentration.

Unfortunately, a quantitative interpretation is hampered by the lack of theoretical models describing the local nanoscale potential as a function of the local carrier concentration. Therefore, as first guess we use a macroscopic model[12] *modified* by replacing the infinitely constant potential and carrier concentrations by spatially varying local quantities, i.e., the local carrier concentration n_{local} and the local potential fluctuations ΔE_C, yielding

$$n_{\text{local}}=\frac{gm_{\text{eff}}kT}{\pi\hbar^2}\ln(1+e^{-(E_{C,\text{avg}}-E_F+\Delta E_C)/kT}). \tag{2}$$

With Eq. (2), the data in Fig. 2(a) can be well fitted (solid line) using the spatially averaged CB edge position relative to the E_F, $E_{C,\text{avg}}-E_F$, and the effective electron mass m_{eff} as fitting parameters. Figure 2(b) shows the effective masses obtained from different data sets and the weighted average of $(0.35\pm0.09)m_0$ (horizontal line) assuming a degeneracy of $g=6$ [electrons in the CB of Si(111)[12]]. This value agrees well with $m_{\text{eff}}=0.37m_0$ for a Si(111)1×1 plane.[12,13] With $g=2$ (CB of the Ga overlayer[14]), m_{eff} would be three times larger and not agree with $0.4m_0$ estimated for the CB of the Ga overlayer.[14] The position of the Fermi level is 0.013 ± 0.010 eV below E_C. Thus, the free electrons induced by the dopants are located in the Si(111) plane underneath the $\sqrt{3}\times\sqrt{3}$ Ga layer (because $E_C<E_{CS}$).[14]

In order to address the limits of the above model, we quantified the lateral extensions of the local potential fluctuations using the 2D power spectrum (PS) and the related autocorrelation function (ACF) of the STM images. The radially integrated 2D PS in Fig. 3(a) shows two exponential decays (F and D) beside a peak at $k=2/(\sqrt{3}\,a)\approx1.74$ nm^{-1} ($a=0.665$ nm) of the atomic lattice (L). This indicates that two separate effects contribute to the nanoscale potential. They can be assigned to long-range potential fluctuations (F) and local 2D screened Coulomb potentials around the charged dopants (D). Fig. 3(b) shows the Lorentzian width of the radially integrated ACF versus the global dopant concentration n_{global} of both contributions. The Lorentzian widths D remain unchanged at ≈0.36 nm. This value fits well to twice the radial screening length (2×0.2 nm) of the 2D screened Coulomb potential, calculated with m_{eff} and E_F obtained above.[12] Thus the contribution D

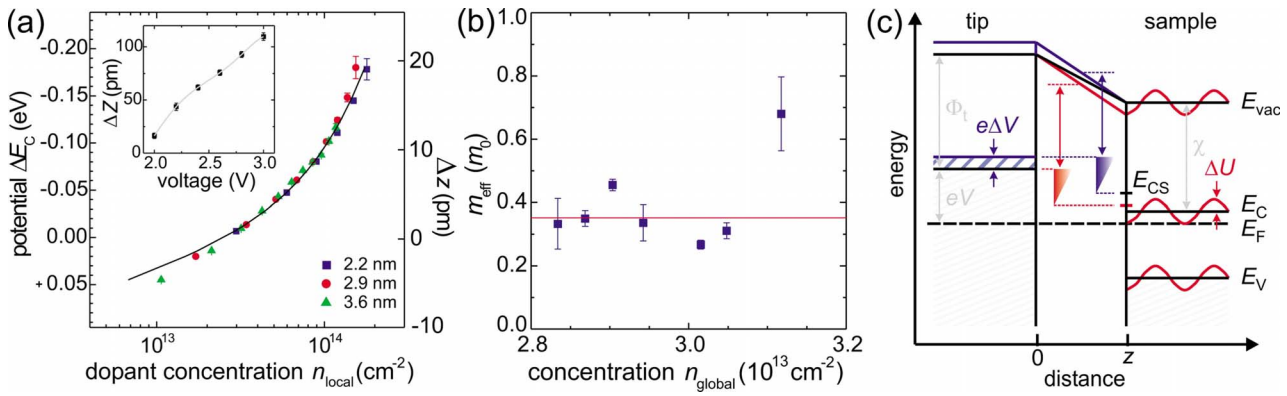

FIG. 2. (Color online) (a) Local deviation from the average potential ΔE_C (left axis) derived from the local height change Δz (right axis) as a function of the local dopant concentration n_{local} for different resolutions. The solid line is a fit to the data. Inset: corresponding height–voltage curve at a set current of 0.1 nA, probing the energy (voltage) sensitivity of the tip. (b) Effective mass m_{eff} vs the global dopant concentration n_{global} obtained from fitting different data sets. (c) Schematics of the tunneling process with varying voltage (marked $e\Delta V$, blue) and spatially varying local potential on the sample (ΔU). The currents are indicated by triangles, respectively. E_{CS} is the CB minimum of the $\sqrt{3}\times\sqrt{3}$ Ga surface.

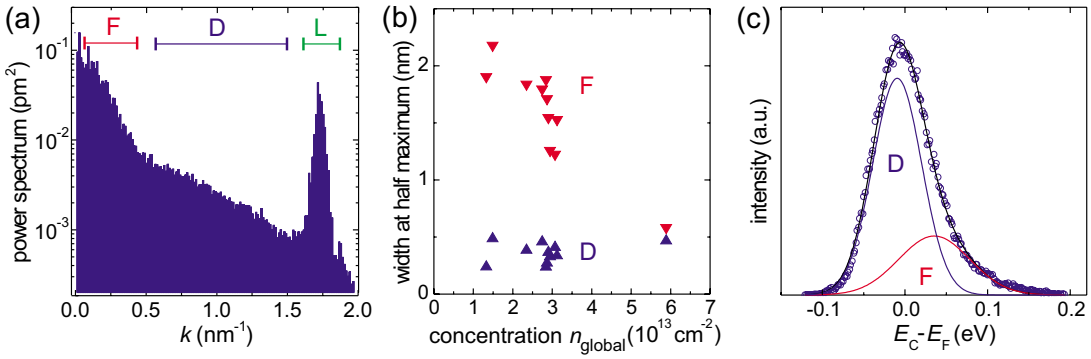

FIG. 3. (Color online) (a) Radially integrated 2D power spectrum. Two exponential decays (F and D) and the peak arising from the atomic lattice (L) are present. (b) Full width at half maximum of the potential fluctuations (F) and the local 2D screened Coulomb potential (D) as a function of the global dopant concentration extracted from the power spectra. The potential fluctuations vanish at high concentrations. (c) Measured distribution of the conduction band edge energy (resolution is 4.3 nm). The distribution is constituted by two Gaussian peaks, originating from the potential fluctuations (F) and the local 2D screened Coulomb potentials (D).

to the nanoscale potential can be attributed to screening due to electron-electron interactions.

In contrast, the widths of the long-range potential fluctuations (F) decrease with the dopant concentration and vanish at $n_{\text{global}} \approx 6 \times 10^{13}$ cm^{-2}. We recall that potential fluctuations are essentially a collection of many n^+-n^{++} interfaces. Their depletion width can be estimated to 0.6–1.1 nm,[15] using a dielectric constant ranging between that of Si (ε_{Si}) and a Si surface $(\varepsilon_{\text{Si}}+1)/2$, 0.15 eV potential difference, and dopant concentrations of 10^{13}–10^{14} cm^{-2}. Only fluctuations in the dopant distribution that are spatially more extended than twice the depletion width (≈1.2–2.2 nm) lead to potential values as described by Eq. (2). This limit can be directly visualized in Fig. 1(b). The smaller, 3-nm-wide area (marked S) shows a weak dark contrast and thus weak potential change, while the 6-nm-wide larger area (L) exhibits a pronounced potential change. With increasing dopant concentrations, the size of the fluctuations decreases and the probability of having dopant fluctuations larger than twice the depletion width vanish. This explains the observed trend of the long-range potential fluctuations in Fig. 3(b).

Finally, the relation between the two physical effects contributing to the nanoscale potential can be determined from the measured probability distribution of the CB edge (E_C) energy [Fig. 3(c)]. For statistically (Poisson) distributed screened Coulomb potentials, one expects a single Gaussian distribution of the CB edge energy.[16] Although our dopants are Poisson distributed, our data is rather constituted of two Gaussian peaks. This is a further indication that two contributions to the nanoscale potential exist, which can be again assigned to the long-range potential fluctuations (F) and the local 2D screened Coulomb potentials (D). Gaussian peak D is localized primarily on the left flank of the Gaussian peak F, where the Fermi energy is near or above E_C. Since the dopants locally reduce the potential $E_C - E_F$, they are primarily localized in areas with a low or negative potential, i.e., on the left flank of peak F. Thus, the nanoscale potential cannot be described by the sum of the local screened Coulomb potentials only. It is rather given by the superposition of the long-range potential fluctuations and the local deviations of the screened Coulomb potentials from their spatial average.

In conclusion, we visualized and quantified how dopant atoms and their spatial distribution affect the local potential at nanometer scale in a 2D semiconductor. We identified two separate physical mechanisms contributing to the nanoscale potential. First, local potential fluctuations arise from the local concentration of charge carriers in the bands governed by nanoscale inhomogeneities in the dopant distribution. This regime disappears if the spatial extend of dopant fluctuations reaches the extension of space charge regions. Second, due to the presence of charged dopants, the nanoscale potential is superimposed by the local deviations of the screened Coulomb potentials from their spatial average. The potential is not the simple sum of all screened Coulomb potentials around charged dopants. These results provide the experimental basis for understanding quantitatively the potential in spatially and dimensionally reduced semiconductor structures and devices.

The authors thank the Deutsche Forschungsgemeinschaft and the GIF for financial support and J. Teng for assistance in part of the data collection.

[1] S. Roy and A. Asenov, Science **309**, 388 (2005).
[2] M. R. Castell, D. A. Muller, and P. M. Voyles, Nature Mater. **2**, 129 (2003).
[3] Ph. Ebert, T. J. Zhang, F. Kluge, M. Simon, Z. Zhang, and K. Urban, Phys. Rev. Lett. **83**, 757 (1999).
[4] N. D. Jäger, K. Urban, E. R. Weber, and Ph. Ebert, Appl. Phys. Lett. **82**, 2700 (2003); N. D. Jäger, K. Urban, E. R. Weber, and Ph. Ebert, Phys. Rev. B **65**, 235302 (2002); S. Perraud, K. Kanisawa, Z.-Z. Wang, and T. Fujisawa, Phys. Rev. B **76**, 195333 (2007).
[5] M. Morgenstern, J. Klijn, C. Meyer, M. Getzlaff, R. Adelung, R. A. Römer, K. Rossnagel, L. Kipp, M. Skibowski, and R. Wiesendanger, Phys. Rev. Lett. **89**, 136806 (2002).
[6] R. J. Hamers and J. E. Demuth, Phys. Rev. Lett. **60**, 2527 (1988).
[7] S. Landrock, Thesis, RWTH Aachen University, 2009.
[8] Ph. Ebert, Surf. Sci. Rep. **33**, 121 (1999), and references therein.
[9] Y. Dong, R. M. Feenstra, R. Hey, and K. H. Ploog, J. Vac. Sci. Technol. B **20**, 1677 (2002).
[10] J. A. Stroscio, R. M. Feenstra, D. M. Newns, and A. P. Fein, J. Vac. Sci. Technol. A **6**, 499 (1988).
[11] The condition that the tunnel current for energies between E_F and $E_F + e\Delta V$ is negligible is fulfilled, since E_F is deeper in the *surface* band gap than $e\Delta V$ and electrons primarily tunnel into the Ga overlayer surface states.
[12] F. Stern and W. E. Howard, Phys. Rev. **163**, 816 (1967).
[13] M. A. Green, J. Appl. Phys. **67**, 2944 (1990).
[14] J. M. Nicholls, B. Reihl, and J. E. Northrup, Phys. Rev. B **35**, 4137 (1987).
[15] A. S. Achoyan, A. E. Yesayan, E. M. Kazaryan, and S. G. Petrosyan, Semiconductors **36**, 903 (2002).
[16] E. O. Kane, Phys. Rev. **131**, 79 (1963); J. M. Rorison, M. J. Kane, D. C. Herbert, M. S. Skolnick, L. L. Taylor, and S. J. Bass, Semicond. Sci. Technol. **3**, 12 (1988).